$0-\pi$ Transitions in a Superconductor/Chiral magnet/Superconductor Junction

Thierry Champel,[1,2] Tomas Löfwander,[1,3] and Matthias Eschrig[1,4]

[1] *Institut für Theoretische Festkörperphysik and DFG-Center for Functional Nanostructures, Universität Karlsruhe, D-76128 Karlsruhe, Germany*
[2] *Laboratoire de Physique et Modélisation des Milieux Condensés, CNRS and Université Joseph Fourier, 25 Avenue des Martyrs, BP 166, F-38042 Grenoble, France*
[3] *Department of Microtechnology and Nanoscience - MC2, Chalmers University of Technology, S-41296 Göteborg, Sweden*
[4] *Fachbereich Physik, Universität Konstanz, D-78457 Konstanz, Germany*

(Dated: June 22, 2007)

We study the π phase in a superconductor-ferromagnet-superconductor Josephson junction, with a ferromagnet showing a cycloidal spiral spin modulation with in-plane propagation vector. Our results reveal a high sensitivity of the junction to the spiral order and indicate the presence of 0-π quantum phase transitions as function of the spiral wave vector. We find that the chiral magnetic order introduces chiral superconducting triplet pairs that strongly influence the physics in such Josephson junctions, with potential applications in nanoelectronics and spintronics.

It is by now well established that an equilibrium superconducting phase difference of π can be arranged between two singlet superconductors when separating them by a suitably chosen ferromagnetic material [1, 2]. Transitions between the π-state and the 0-state of such S-F-S Josephson junctions have been revealed in experiments through oscillations of the Josephson critical current with varying thickness of the ferromagnet [3] or with varying temperature [4]. The π Josephson junction is currently of considerable interest as an element complementary to the usual Josephson junction in the development of functional nanostructures [5], including superconducting electronics [6] and quantum computing [7].

Recently, there has been a rapid progress in the field of chiral magnetism [8, 9, 10, 11] that raises the expectations for applications of chiral magnets in spintronics. Chiral order occurs in inversion asymmetric magnetic materials [9, 11] that in the presence of spin-orbit coupling give rise to a Dzyaloshinskii-Moriya interaction $\mathbf{D}_{ij}\cdot(\mathbf{S}_i\times\mathbf{S}_j)$. This interaction favors a directional noncollinear (spiral) spin structure of a specific chirality over the usual collinear arrangement favored by the Heisenberg exchange interaction $J_{ij}(\mathbf{S}_i\cdot\mathbf{S}_j)$. A well-studied [10, 11] chiral magnet is the transition-metal compound MnSi, with the spiral wave length $\Lambda\approx 180$ Å. Nanoscale magnets or magnetic systems with reduced dimensionality that frequently lack inversion symmetry due to interfaces and surfaces are expected to exhibit chiral magnetism [8]. This has been confirmed by the recent observation [9] of a spin spiral structure (with $\Lambda\approx 12$ nm) in a single atomic layer of manganese on a tungsten substrate.

In this Letter, we combine chiral magnetism with superconductivity in a controllable Josephson nano-device where $0-\pi$ transitions can be induced by tuning the magnetic spiral wave vector Q (see Fig. 1). Whereas in bulk magnets Q can be manipulated e.g. by means of pressure, in nano-magnets alternative possibilities of control exist, as electric fields, geometry, or pinning layers. Such a Josephson device shows a surprisingly complex behavior with 0- to π-state transitions as function of spiral wave length $\Lambda=2\pi/Q$, that turn into zero temperature transitions for some critical wave vectors. However, below the threshold $\Lambda_{\rm th}=\pi\xi_J$, where ξ_J is the penetration depth of pairs into the chiral magnet (ξ_J depends on material constants), a qualitatively different behavior is found.

Within our model chiral magnetism and singlet superconductivity take place in mutually separated materials, and the magnetic spiral affects only the superconducting proximity amplitudes. This is in contrast to the case of coexisting superconducting and spiral magnetic order in the same material, e.g. in ferromagnetic superconductors [12]. We also contrast our model to the case of a helical spiral spin modulation with a propagation wave vector perpendicular to the S-F interface [13], and the Josephson effect in S-F-S junctions with a Néel domain structure [14]. The physics studied in Refs. [13, 14] is dominated by the presence of long-range triplet components, that are absent in the present system [15] (concerning the role of long-range triplet pairs in S-F-S hybrid structures see also [16]). In Refs. [13, 14], a strong dependence of the Josephson critical current I_c on the ferromagnet inhomogeneity is found due to these long-

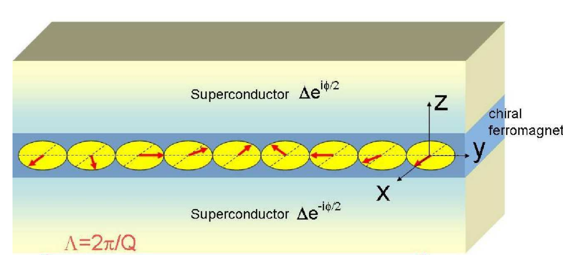

FIG. 1: (Color online) S-CM-S Josephson junction where CM is a chiral ferromagnet with a cycloidal spiral spin modulation, i.e. the spins are confined to a plane (the $x-y$-plane) parallel to the spiral propagation direction (the y-axis).

range components. However, the related magnitude of I_c is so small that the observation of such an effect is questionable. In this paper, we report a critical current with a much larger magnitude [17], which is essential for potential applications.

We study the S-CM-S junction shown in Fig. 1 within the framework of the quasiclassical theory of superconductivity and consider the diffusive limit. Furthermore, we shall assume that the pair correlations induced in the chiral magnet, quantified by the anomalous Green function f, are small. This is fulfilled for temperatures close to the superconducting critical temperature T_c, and also for much smaller temperatures T provided that the S-CM interface transparency is small. We decompose the 2×2 spin-matrix f as $f = f_s i\sigma_y + i(\mathbf{f}_t \cdot \boldsymbol{\sigma})\sigma_y$, where f_s is the singlet component and $\mathbf{f}_t$ is the triplet vector (here $\boldsymbol{\sigma} = (\sigma_x, \sigma_y, \sigma_z)$ is a vector of Pauli matrices). These components obey [15] in the magnet a system of linearized Usadel equations

$$
\begin{aligned}
(D\boldsymbol{\nabla}^2 - 2\varepsilon_n) f_s &= 2i\mathbf{J} \cdot \mathbf{f}_t, && (1)\\
(D\boldsymbol{\nabla}^2 - 2\varepsilon_n) \mathbf{f}_t &= 2i\mathbf{J} f_s, && (2)
\end{aligned}
$$

where $\varepsilon_n = \pi T(2n+1)$ is the Matsubara frequency with n a positive integer. Quantities for negative frequencies are obtained through symmetry relations [15], the components f_s and $\mathbf{f}_t$ being respectively even and odd in ε_n. The z-axis is perpendicular to the interfaces, and the CM region is delimited by $|z| < d_f/2$, where d_f is the thickness of the CM layer. The exchange field $\mathbf{J}$ is nonzero in the CM region, while the singlet superconducting order parameter Δ_s is nonzero only in the S regions. The S and CM parts can have different diffusion constants, D_s and D_f, and therefore also different superconducting coherence lengths $\xi_{s,f} = \sqrt{D_{s,f}/2\pi T_c}$. For simplicity, we assume that the two S regions, and also the two S/CM interfaces, are characterized by identical parameters. Another important length scale is the magnetic length $\xi_J = \sqrt{D_f/J}$.

The exchange field $\mathbf{J}$ rotates within the $x-y$ plane in the CM film with a spiral wave vector $Q\mathbf{e}_y$,

$$\mathbf{J}(y) = J(\cos Qy, \sin Qy, 0). \tag{3}$$

As a result f depends on both spatial coordinates z and y. The triplet vector $\mathbf{f}_t$ is found to be parallel to $\mathbf{J}$ everywhere [15]. It is convenient to introduce chiral triplet components $f_\pm = (\mp f_{tx} + i f_{ty})\, e^{\pm iQy}$. In the CM layer, the singlet component f_s and the two chiral triplet components $f_\pm$ are then given by

$$f_l(z) = \sum_{\epsilon=\pm 1} \varphi_{l,\epsilon} \left[a_\epsilon \cosh(k_\epsilon z) + b_\epsilon \sinh(k_\epsilon z)\right], \tag{4}$$

where $l = s$ or $\pm$, $\varphi_{s,\epsilon} = \eta_\epsilon$, $\varphi_{-,\epsilon} = \epsilon$, $\varphi_{+,\epsilon} = -\epsilon$ and

$$k_\epsilon = \sqrt{2(\varepsilon_n + \epsilon i J \eta_{-\epsilon})/D_f}, \tag{5}$$

$$\eta_\epsilon = \begin{cases} \sqrt{1-\eta^2} + i\epsilon\eta & \text{for} \quad \eta \le 1 \\ -i(\sqrt{\eta^2 - 1} - \epsilon\eta) & \phantom{\text{for}} \quad \eta > 1 \end{cases}, \tag{6}$$

where $\eta = D_f Q^2/4J = (Q\xi_J)^2/4$. As the singlet component f_s, the chiral triplet components penetrate over the short length scale ξ_J inside the chiral magnet.

The different coefficients a_ϵ and b_ϵ are determined by boundary conditions for the two S/CM interfaces (located at $z = \pm d_f/2$). These connect the f on the S side of the interface (denoted z_s) with the f on the CM side at the interface (denoted z_f) and read [18]

$$
\begin{aligned}
\gamma \xi_f \partial_z f_l(z_f) &= \xi_s \partial_z f_l(z_s), && (7)\\
\gamma_b \xi_f \partial_z f_l(z_f) &= \pm\left[f_l(z_s) - f_l(z_f)\right], && (8)
\end{aligned}
$$

for the triplet ($l = \pm$) and singlet ($l = s$) amplitudes. The parameters γ and γ_b are related to the conductivity mismatch between the two sides ($\gamma\xi_f/\xi_s = \sigma_f/\sigma_s$ with the bulk conductivities σ_f in CM and σ_s in S) and the boundary resistance, respectively. The signs $\pm$ in Eq. (8) refer to the interfaces at $z = \pm d_f/2$, respectively. In the following, we define the short-hand notation $\delta^{(\pm)} = f_s(\pm d_f/2)$ for the singlet amplitudes at the interfaces.

Due to the leakage of pair correlations into the central CM region, the amplitudes $\delta^{(\pm)}$ are expected to be reduced compared with the bulk value in S. This inverse proximity effect can be important in hybrid structures involving ferromagnets (see e.g. Ref. 19). However, the spatial dependences of f_s as well as of the triplet components can be disregarded in S when $\gamma \ll 1+\gamma_b d_f/\xi_f$, and the rigid boundary conditions hold (see, e.g., Ref. [1]), with $\delta^{(\pm)} \approx \pi\Delta_s e^{\pm i\phi/2}/\sqrt{\varepsilon_n^2 + \Delta_s^2}$, where ϕ is the phase difference between the two superconductors. Using Eqs. (7)-(8) within this assumption, we express a_ϵ and b_ϵ as functions of $\delta^{(\pm)}$

$$
\begin{aligned}
a_\epsilon &= \frac{\delta^{(+)} + \delta^{(-)}}{2} \, \frac{1}{(\eta_\epsilon + \eta_{-\epsilon})\, \mathcal{A}_\epsilon}, && (9)\\
b_\epsilon &= \frac{\delta^{(+)} - \delta^{(-)}}{2} \, \frac{1}{(\eta_\epsilon + \eta_{-\epsilon})\, \mathcal{B}_\epsilon}, && (10)
\end{aligned}
$$

where $\mathcal{A}_\epsilon = \cosh(x_\epsilon) + \gamma_b k_\epsilon \xi_f \sinh(x_\epsilon)$, $\mathcal{B}_\epsilon = \sinh(x_\epsilon) + \gamma_b k_\epsilon \xi_f \cosh(x_\epsilon)$, and $x_\epsilon = k_\epsilon d_f/2$.

The current flowing through the S-CM-S junction is

$$I = 2e\frac{D_f}{\pi} N_f \mathcal{S} T \sum_n \operatorname{Im}\left[f_s^* \partial_z f_s - f_{tx}^* \partial_z f_{tx} - f_{ty}^* \partial_z f_{ty}\right], \tag{11}$$

where N_f is the Fermi-level density of states per spin in CM and $\mathcal{S}$ is the cross-section area. We insert $f_{tx}^* \partial_z f_{tx} + f_{ty}^* \partial_z f_{ty} = \left(f_-^* \partial_z f_- + f_+^* \partial_z f_+\right)/2$ and Eq. (4) in Eq. (11), and express I as a function of a_ϵ and b_ϵ as

$$I = 4e\frac{D_f}{\pi} N_f \mathcal{S} T \sum_{n\ge 0} \sum_{\epsilon,\epsilon'} \operatorname{Im}\left[(\eta_{\epsilon'}^* \eta_\epsilon - \epsilon'\epsilon) a_{\epsilon'}^* b_\epsilon k_\epsilon\right]. \tag{12}$$

For $\eta < 1$ only the terms with $\epsilon \neq \epsilon'$ contribute, while for $\eta > 1$ only the terms with $\epsilon = \epsilon'$ contribute [the case

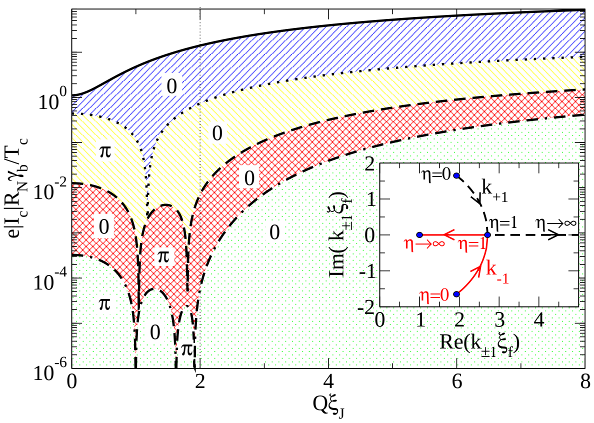

FIG. 2: (Color online) Josephson critical current I_c versus the spiral wave vector Q for a few thicknesses of the ferromagnet: curves from top to bottom $d_f/\xi_f = 0.1,\ 1,\ 3,\ 5$. Here $T = 0.1T_c$ and $J = 20T_c$. The inset shows the flow of the real and imaginary parts of the eigenvalues $k_{\pm 1}$ with varying $\eta = (Q\xi_J)^2/4$ for $\varepsilon_n = \pi T_c$.

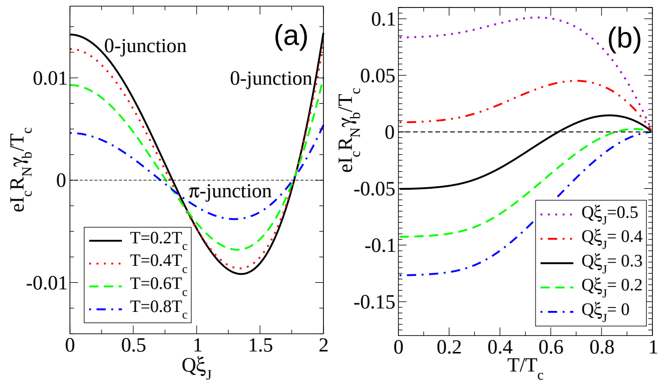

FIG. 3: (Color online) (a) Critical current versus spiral wave vector for a few temperatures, in the region $0 \le Q\xi_J \le 2$ where $0-\pi$ transitions are possible. Here $d_f = 2.7\xi_f$ and $J = 20T_c$. (b) The $0-\pi$ transition is observable as function of temperature for a certain thickness (here $d_f = 0.45\xi_f$) by tuning the spiral wave vector. The other model parameters are the same as in (a).

$\eta = 1$ is defined via the corresponding limit in Eq. (12)]. In agreement with current conservation, the dependence on z vanishes.

It then follows from Eqs. (9), (10), and (12) that the current-phase relation reduces to sinusoidal form $I = I_c \sin(\phi)$. Close to T_c we get for I_c

$$I_c R_N = 4V_0 \left(\frac{d_f}{\xi_f} + 2\gamma_b\right) \sum_{n\geq 0} \sum_{\epsilon=\pm 1} \frac{T_c^2}{\varepsilon_n^2} \frac{k_\epsilon \xi_f \eta_\epsilon}{\mathcal{A}_\epsilon \mathcal{B}_\epsilon (\eta_\epsilon + \eta_{-\epsilon})}, \tag{13}$$

where $R_N = (d_f + 2\gamma_b\xi_f)/\sigma_f \mathcal{S}$ is the normal state resistance, $\sigma_f = 2e^2 N_f D_f$ is the conductivity of the CM layer, and $V_0 = \pi\Delta_s^2/4eT_c$. On the other hand, for low barrier transparencies ($\gamma_b \gg 1$) [20], we have $\mathcal{A}_\epsilon \approx \gamma_b k_\epsilon \xi_f \sinh(k_\epsilon d_f/2)$ and $\mathcal{B}_\epsilon \approx \gamma_b k_\epsilon \xi_f \cosh(k_\epsilon d_f/2)$, which lead to

$$I_c R_N = \frac{4\pi}{\gamma_b} \frac{T}{e} \sum_{n\geq 0} \sum_{\epsilon=\pm 1} \frac{\Delta_s^2}{\varepsilon_n^2 + \Delta_s^2} \frac{\eta_\epsilon/(\eta_\epsilon + \eta_{-\epsilon})}{k_\epsilon \xi_f \sinh(k_\epsilon d_f)}. \tag{14}$$

In the absence of inhomogeneity ($Q = 0$), we then recover expressions for the critical current in the literature [1]. Note that the temperature T appears through several terms in Eq. (14), such as Δ_s (here we assume the BCS temperature dependence), ε_n and k_ϵ.

In the following we study the influence of an exchange field with chiral order on the Josephson effect on the basis of Eq. (14). For small thicknesses d_f we have used the more general expression (12) to verify that Eq. (14) indeed is applicable in the parameter range we consider. As we show in Fig. 2, the chiral magnetic order introduces a surprizingly rich behavior: the magnitude of I_c as function of increasing wave vector Q presents initial oscillations and suppression, followed by increase and final saturation. Depending on the thickness of the CM layer, there can be one or several $0-\pi$ and $\pi-0$ transitions as function of the spiral order wave vector Q. Above a certain value of Q ($Q\xi_J = 2$ indicated by the vertical line in the figure) I_c is positive independently of other model parameters, meaning that the junction phase difference is stabilized at zero. Physically, this can be understood as an averaging out of the exchange field within one magnetic length ξ_J. Technically, this critical value of Q separates a region with complex eigenvalues k_ϵ ($\eta < 1$, oscillating I_c) from a region with real k_ϵ ($\eta > 1$, monotonously increasing I_c), see the inset of Fig. 2. For $\eta < 1$, the complex k_ϵ leads to a non-monotonic dependence of I_c as function of Q. In the large-Q limit, the Josephson critical current for a junction with a normal metal is recovered.

In Fig. 3(a) we study in more detail the critical current within the region $0 \le Q\xi_J \le 2$ supporting oscillations. For an intermediately thick magnetic film (here $d_f = 2.7\xi_f$) it is possible to see both $0-\pi$ and $\pi-0$ transitions as function of Q, with a reasonably large critical current. The phase transitions shift to lower values of Q with increasing temperature. As seen in Fig. 3(b), the spiral order can also induce $0-\pi$ transitions as function of temperature for certain parameter ranges.

Phase-diagrams of the $\pi-0$ transitions are presented in Fig. 4. We see that in the low-T region [panel (a)] the phase transition line $T_{\pi-0}(Q)$ develops a very steep slope. This insensitivity to temperature variations can be of importance for device applications. Although at ultra-low temperatures a more sophisticated theory than the mean field approach presented here should be used, our results in Fig. 4 give a strong indication of a $\pi-0$ transition as a function of Q also at zero temperature. Thus, the system of a chiral magnet sandwiched between two superconductors is of potential interest for the study

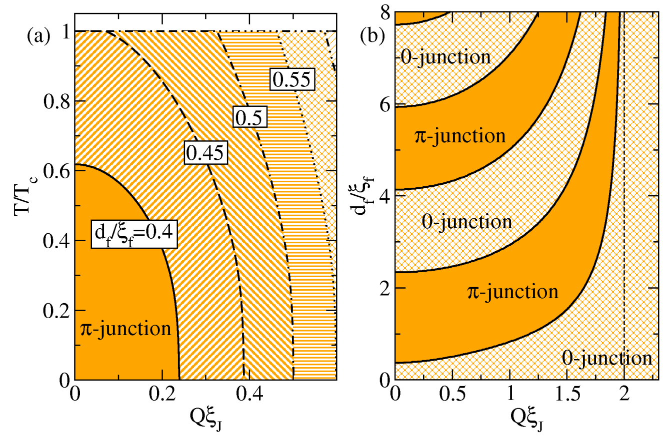

FIG. 4: (Color online) (a): (T-Q) phase diagram for a Josephson junction with a chiral magnet ($J = 20T_c$) between two singlet superconductors. The transition from a π-junction at smaller chiral wave vector Q to a 0-junction at larger Q is indicated for several thicknesses of the ferromagnetic layer. (b): corresponding low-T (d_f-Q) phase diagram ($T = 0.1T_c$).

of critical behavior near a quantum critical point.

In the right panel of Fig. 4 the very different behaviors for $Q\xi_J < 2$ and > 2 are also seen. For $Q\xi_J < 2$ the spiral order shifts the transition lines towards thicker magnetic films, but the transition line never disappears from the phase diagram. Only in the region $Q\xi_J > 2$ is the averaging of the exchange field over the magnetic length so effective as to prevent $0 - \pi$ transitions.

In summary, we have studied the Josephson effect in an S-CM-S junction in the presence of an in-plane cycloidal spin spiral structure in the magnet. We have found that the presence of a spin spiral can change the ground state of the Josephson junction, and lead to a transition between a π-junction and a 0-junction for a critical spiral wave vector. The dependences of the Josephson effect on magnet thickness and on temperature depend sensitively on the wave vector of the chiral order in the magnet. We predict that a quantum-critical point should exist in the phase-diagram for suitably chosen sample parameters. We expect that these effects will have potential applications for new types of functional nanoscale structures. The ultimate goal for the future is to tune Josephson junctions with one or more chiral magnets by controlling the phases or magnitudes of the spiral magnetic wave vectors.

We would like to thank Gerd Schön for valuable contributions to this work. T.L. acknowledges support from the Alexander von Humboldt Foundation.

Note added. - After submission, we became aware of work by Crouzy *et al.* [21], who study in-plane magnetic Néel domain walls. Their model is markedly different from ours, but leads to similar findings about the periodicity of 0 to π transitions with the magnetic inhomogeneity.

[1] A. A. Golubov, M. Yu. Kupriyanov, and E. Il'ichev, Rev. Mod. Phys. **76**, 411 (2004); A. I. Buzdin, Rev. Mod. Phys. **77**, 935 (2005); F.S. Bergeret, A.F. Volkov, and K.B. Efetov, Rev. Mod. Phys. **77**, 1321 (2005).
[2] P. H. Barsic, O. T. Valls, and K. Halterman, Phys. Rev. B **75**, 104502 (2007); Z. Pajovic *et al.*, Phys. Rev. B **74**, 184509 (2006); B. Crouzy, S. Tollis, and D. A. Ivanov, Phys. Rev. B **75**, 054503 (2007).
[3] T. Kontos *et al.*, Phys. Rev. Lett. **89**, 137007 (2002); Y. Blum *et al.*, Phys. Rev. Lett. **89**, 187004 (2002); W. Guichard *et al.*, Phys. Rev. Lett. **90**, 167001 (2003); V. A. Oboznov *et al.*, Phys. Rev. Lett. **96**, 197003 (2006); V. Shelukhin *et al.*, Phys. Rev. B **73**, 174506 (2006); J. W. A. Robinson *et al.*, Phys. Rev. Lett. **97**, 177003 (2006).
[4] V. V. Ryazanov *et al.*, Phys. Rev. Lett. **86**, 2427 (2001); H. Sellier *et al.*, Phys. Rev. Lett. **92**, 257005 (2004); S. M. Frolov *et al.*, Phys. Rev. B **70**, 144505 (2004).
[5] J.J.A. Baselmans *et al.*, Nature **397**, 43 (1999).
[6] T. Ortlepp *et al.*, Science **312**, 1495 (2006).
[7] L.B. Ioffe *et al.*, Nature **415**, 503-506 (2002).
[8] A.N. Bogdanov and U.K. Rößler, Phys. Rev. Lett. **87**, 037203 (2001).
[9] M. Bode *et al.*, Nature **447**, 190 (2007).
[10] B. Binz, A. Vishwanath, and V. Aji, Phys. Rev. Lett. **96**, 207202 (2006); S.V. Maleyev, Phys. Rev. B **73**, 174402 (2006); D. Belitz, T.R. Kirkpatrick, and A. Rosch, Phys. Rev. B **73**, 054431 (2006).
[11] C. Thessieu *et al.*, J. Phys.: Condens. Matter **9**, 6677 (1997); C. Pfleiderer *et al.*, Nature **427**, 227 (2004).
[12] M.L. Kulić and I.M. Kulić, Phys. Rev. B **63**, 104503 (2001); I. Eremin, F.S. Nogueira, and R.-J. Tarento, Phys. Rev. B **73** 54507 (2006); J. Linder, M. S. Grønsleth, and A. Sudbø, Phys. Rev. B **75** 54518 (2007).
[13] F.S. Bergeret, A.F. Volkov, and K.B. Efetov, Phys. Rev. B **64**, 134506 (2001); A.F. Volkov, A. Anishchanka, and K.B. Efetov, Phys. Rev. B **73**, 104412 (2006).
[14] Ya. V. Fominov, A. F. Volkov, and K. B. Efetov, Phys. Rev. B **75**, 104509 (2007).
[15] T. Champel and M. Eschrig, Phys. Rev. B **71**, 220506(R) (2005); **72**, 054523 (2005).
[16] M. Eschrig *et al.*, Phys. Rev. Lett. **90**, 137003 (2003); F. S. Bergeret, A. F. Volkov, and K. B. Efetov, Phys. Rev. B **68**, 064513 (2003); T. Löfwander *et al.*, Phys. Rev. Lett. **95**, 187003 (2005) ; A. F. Volkov, Ya. V. Fominov, and K. B. Efetov, Phys. Rev. B **72**, 184504 (2005); A. Konstandin, J. Kopu, and M. Eschrig, Phys. Rev. B **72**, 140501(R) (2005); Y. Asano, Y. Tanaka, and A.A. Golubov, Phys. Rev. Lett. **98**, 107002 (2007); V. Braude and Yu.V. Nazarov, Phys. Rev. Lett. **98**, 077003 (2007).
[17] The magnitude of I_c is in our case [see Eqs.(13)-(14) below] not characterized by a small prefactor $\propto \xi_J^2 Q/\xi_f$ or $\xi_J^4 Q^3/\xi_f$ in strong contrast to formulas derived in Refs. [13] and [14], respectively.
[18] M. Yu. Kupriyanov and V. F. Lukichev, Sov. Phys. JETP **67**, 1163 (1988).
[19] T. Löfwander, T. Champel, and M. Eschrig, Phys. Rev. B **75**, 014512 (2007).
[20] We assume that the following inequalities hold $(\gamma_b k_\epsilon \xi_f)^{-1} \ll \tanh(x_\epsilon) \ll \gamma_b k_\epsilon \xi_f$.
[21] B. Crouzy, S. Tollis, and D.A. Ivanov, Phys. Rev. B **76**, 134502 (2007).